Acta Mathematicae Applicatae Sinica, English Series
Vol. 32, No. 4 (2016) 969–982
DOI: 10.1007/s10255-016-0618-1
http://www.ApplMath.com.cn & www.SpringerLink.com

Acta Mathematicae Applicatae Sinica, English Series

An Analysis of Two Variational Models for Speckle Reduction of Ultrasound Images

Zheng-meng JIN[1], Xiao-ping YANG[2,†]

[1]School of Science, Nanjing University of Posts and Telecommunications, Nanjing 210046, China
(E-mail: jinzhm@njupt.edu.cn)
[2]School of Science, Nanjing University of Science and Technology, Nanjing 210094, China
(E-mail: yangxp@mail.njust.edu.cn)

Abstract In this paper, we consider two variational models for speckle reduction of ultrasound images. By employing the Γ-convergence argument we show that the solution of the SO model coincides with the minimizer of the JY model. Furthermore, we incorporate the split Bregman technique to propose a fast alterative algorithm to solve the JY model. Some numerical experiments are presented to illustrate the efficiency of the proposed algorithm.

Keywords BV; Γ-convergence; equivalence; multiplicative noise; Split Bregman algorithm
2000 MR Subject Classification 68U10; 49J40; 65K10

1 Introduction and Main Results

Multiplicative noises (also known as speckle noises) are commonly found in coherent imaging systems, such as synthetic aperture radar (SAR), sonar, ultrasonic and laser imaging. This paper focus on the speckle noise removal problems in ultrasound images. Let f be an observed image with multiplicative noises defined on Ω, where $\Omega \subset \mathbb{R}^2$ is connected and bounded with Lipschitz boundary. The multiplicative noise model is given by

$$f = un, \tag{1.1}$$

where u denotes the image to be recovered and n is the noise. Without loss of generality, we can assume that f, u and n are positive in the noise model. Unlike additive noises, these noises are much more difficult to be removed from the corrupted images, mainly because of not only their multiplicative nature, but also their distributions which are generally not Gaussian.

As far as we know, the variational approach devoted to multiplicative noise is firstly proposed by Rudin, Lions and Osher[16]. In [16], under the assumption that the mean of the multiplicative noise is equal to 1 and the variance is known, the authors introduced the following denoising model:

$$\min_u \Big\{ J(u) + \lambda \int_\Omega \frac{f}{u} + \mu \int_\Omega \Big(\frac{f}{u} - 1\Big)^2 \Big\}, \tag{1.2}$$

where $J(u) := \int_\Omega |Du|$ is the TV regularization term, the last two terms are the data fitting terms, λ and μ are the weighted parameters. Numerical experiment results show that this model

Manuscript received March 20, 2012. Revised July 10, 2013.
Supported by the National Natural Science Foundation of China under Grants No. 11671004 and 91330101, and Natural Science Foundation for Colleges and Universities in Jiangsu Province under Grants No. 15KJB110018 and 14KJB110020.
†Corresponding author.

is effective for the Gaussian multiplicative noise. Recently multiplicative noise removal problems have attracted much attention. In [1], based on maximum a posteriori (MAP) regularization approach, Aubert and Aujol derived the denoising model (called AA model) as follows:

$$\min_u \Big\{ J(u) + \lambda \int_\Omega (\log u + \frac{f}{u}) \Big\}, \tag{1.3}$$

where the last term is the fitting term, λ is the weighted parameter. AA Model (1.3) is specifically devoted to the denoising of images corrupted by Gamma multiplicative noise. The authors of [1] proved the existence of a minimizer to the variational Problem (1.3), and derived existence and uniqueness results of the solution to the associated evolution problem. One of the drawbacks of the objective functional in (1.3) is that it is not globally convex for all u, it may lead to that the computed solution by some optimization methods is not a global optimal solution for (1.3). In order to overcome this drawback, the authors of [18] proposed a convex variational model. Indeed, they considered a more general data fitting term, which includes the RLO Model (1.2) and the following Model (1.4). Additionaly, some theoretical analysis and numerical algorithm study about these models can be found in [2,11,19].

In ultrasound images the speckle noise commonly follows a Rayleigh distribution and satisfies the multiplicative noise Model (1.1) (see [21]). The density function of the Rayleigh distribution is given by

$$p(x) = \frac{x}{\sigma^2} \exp\Big(-\frac{x^2}{2\sigma^2} \Big) \mathbf{1}_{\{x \geq 0\}},$$

where $\sigma > 0$ is a parameter. A TV denoising model based on the Rayleigh distribution was proposed by using Markov Random Fields (MRFs) in [3] as follows:

$$\min_u \Big\{ J(u) + \lambda \int_\Omega \Big(2 \log u + \frac{f^2}{u^2} \Big) \Big\}.$$

This model also has the drawback that the data fitting term is not globally convex for all u. Subsequently, by setting $w = \log u$ in the above model Shi and Osher[18] introduced a convex variational model as follows:

$$\begin{aligned} \widehat{w} &= \operatorname{argmin}_w \Big\{ J(w) + \lambda_1 \int_\Omega (2w + f^2 e^{-2w}) \Big\}, \\ u &= e^{\widehat{w}}, \end{aligned} \tag{1.4}$$

where λ_1 is the weighted parameter. They further applied a corresponding relaxed inverse scale space flow to solve this model. In fact, this model can be deduced by using the MAP regularization approach (see the Appendix). Here we call the Model (1.4) as SO model.

In speckle reduction of ultrasound images, one problem should be addressed is that the displayed images from the ultrasound device have been processed by a logarithmic compression algorithm to enhance the weak backscatters[13]. Hence, the speckle noise in the displayed images no longer follows the Rayleigh distribution. Experimental measurements in [15] indicate that the displayed ultrasonic images can be modeled as corrupted with signal-dependent noise of the form:

$$f = u + \sqrt{u} n, \tag{1.5}$$

where n is a zero-mean Gaussian variable. Based on the above fact and the TV regularization, the authors proposed in [12] the following model for removing the speckle noise:

$$\min_{u>0} \Big\{ J(u) + \lambda_2 \int_\Omega \frac{(f-u)^2}{u} \Big\}. \tag{1.6}$$

They further proved the existence uniqueness of a minimizer to the variational Problem (1.6), and derived existence and uniqueness results of the solution to the associated evolution problem. Here we call the Model (1.6) as JY model.

In this paper, motivated by the fact that the SO Model (1.4) and the JY model can be effectively used for speckle reduction of ultrasonic images, we study the relation between these two models. We show that the solution of the SO model coincides with the minimizer of the JY model in the sense of Γ-convergence. Moreover, since the traditional gradient descent algorithm used to solve the JY model in [12] is relatively slow. Here we develop a fast iterative algorithm to solve the JY model by applying the split Bregman technique[10].

This paper is organized as follows. In Section 2 we give some notations of this paper and present some classical theory for the space of $BV(\Omega)$ and Γ-convergence. In Section 3, firstly, the existence and uniqueness of the minimizers to the variational Models (1.4) and (1.6) are proved respectively. Then we employ Γ-convergence argument to get the relation of the solutions to these two models. In Section 4, by incorporating the split Bregman method we propose a fast iterative algorithm to solve the JY model. Some numerical experiments are presented to illustrate the efficiency of the proposed algorithm for speckle noise removal. Finally, we give a conclusion in Section 5.

2 Preliminaries

Let Ω be an open, bounded domain of $\mathbb{R}^2$ with Lipschitz boundary and $f \in L^\infty(\Omega)$. Write $f_{\min} := ess\inf_x f(x)$ and $f_{\max} := ess\sup_x f(x)$. Throughout this paper we restrict our attention to function $f \in L^\infty(\Omega)$ with $f_{\min} > 0$.

Consider the integrands $\varphi, \psi : \Omega \times \mathbb{R} \to [0, +\infty]$ defined by

$$\varphi(x,s) := 2s + f(x)^2 e^{-2s} - 2\log f(x) - 1, \tag{2.1}$$

$$\psi(x,s) := \begin{cases} \dfrac{(f(x)-s)^2}{s}, & \text{for } \ s > 0, \\ +\infty, & \text{otherwise.} \end{cases} \tag{2.2}$$

It is obvious that for fixed $x \in \Omega$, the functions φ and ψ have their minimum at $s = \log f$ and $s = f$, respectively. For these two functions, properties like continuity, lower semi-continuity (l.s.c.), convexity and subdifferentiability are understood with respect to the second variable s. The functionals S_φ, S_ψ are defined by

$$S_\varphi(w) := \int_\Omega \varphi(x, w(x))dx,$$
$$S_\psi(u) := \int_\Omega \psi(x, u(x))dx.$$

It is clear that S_φ and S_ψ are proper and strictly convex, since $\varphi(x,\cdot)$ and $\psi(x,\cdot)$ are normal and strictly convex. Furthermore, by the definition of subdifferential in [7] we get that

$$\partial S_\varphi(w) = \begin{cases} 2(1 - f^2 e^{-2w}), & \text{for } \ 1 - f^2 e^{-2w} \in L^\infty, \\ \emptyset, & \text{otherwise,} \end{cases}$$

$$\partial S_\psi(u) = \begin{cases} 1 - \dfrac{f^2}{u^2}, & \text{for } \ u > 0 \ \text{ a.e. and } \ 1 - \dfrac{f^2}{u^2} \in L^\infty, \\ \emptyset, & \text{otherwise.} \end{cases}$$

Thus, one has that $\partial S_\varphi(w) = 2\partial S_\psi(e^w)$. From now on we always write $T_\varphi, T_\psi : BV(\Omega) \to [0, +\infty]$ by

$$T_\varphi(w) := J(w) + \lambda_1 S_\varphi(w), \qquad T_\psi(u) := J(u) + \lambda_2 S_\psi(u), \tag{2.3}$$

where$\lambda_1, \lambda_2 > 0$ and $J(u) := \int_\Omega |Du|$.

In the following we recall some basic notations and facts on the space of $BV(\Omega)$ (see [8,9,14]).

Definition 2.1. *Define $BV(\Omega)$ as a space of functions $u \in L^1(\Omega)$ such that the following quantity*

$$\int_\Omega |Du| := \sup\Big\{ \int_\Omega u div(\varphi)dx | \varphi \in C_0^1(\Omega;\mathbb{R}^n), |\varphi| \le 1\Big\}$$

is finite. $BV(\Omega)$ is a Banach space with the norm $\|u\|_{BV(\Omega)} = \int_\Omega |Du| + \|u\|_{L^1(\Omega)}$.

About the lower semicontinuity and compactness, we state the following theorems[8].

Theorem 2.1. *suppose $u_k \in BV(\Omega)$ $(k = 1, \cdots)$ and $u_k \to u$ in $L^1_{\rm loc}(\Omega)$. Then*

$$\int_\Omega |Du| \le \liminf_{k\to\infty} \int_\Omega |Du_k|.$$

Theorem 2.2. *Assume $\{u_k\}_{k=1}^\infty$ is a sequence in $BV(\Omega)$ satisfying $\sup_k \|u_k\|_{BV(\Omega)} < \infty$. Then there exists a subsequence $\{u_{k_j}\}_{j=1}^\infty$ and a function $u \in BV(\Omega)$ such that*

$$u_{k_j} \longrightarrow u \qquad in \;\; L^1(\Omega)$$

as $j \to \infty$.

Let us give the definition and some main properties of Γ-convergence[6]. Assume that X is a separable Banach space, endowed with a τ-topology.

Definition 2.2 (Γ-convergence). *Let $F_h : X \to \overline{R}$ be a sequence of functionals. We say that F_h Γ-converge to F for the topology τ if:*

(i) For every x in X and for every sequence x_h τ-converging to x in X,

$$F(x) \le \varliminf_{h\to+\infty} F_h(x_h).$$

(ii) For every x in X there exists a sequence x_h τ-converging to x in X such that

$$F(x) \ge \varlimsup_{h\to+\infty} F_h(x_h).$$

The functional F is called the Γ-limit of F_h and we write $F = \Gamma - \lim F_h$.

Theorem 2.3 (Γ-convergence and Pointwise Convergence).

(i) If F_h converges to F uniformly, then F_h Γ-converges to F.

(ii) If F_h is a decreasing sequence converging to F pointwise, then F_h Γ-converges to RF, the lower semicontinuous envelope of F.

Theorem 2.4. *Assume that F_h is equicoercive and Γ-converges to F. Suppose that F has a unique minimum x_0 in X. If x_h is a sequence in X such that x_h is a minimum for F_h, then x_h converges to x_0 in X and $F_h(x_h)$ converges to $F(x_0)$.*

In the following we list some important results that will be used in the latter section.

Proposition 2.5[19]**.** *(i) Let $f : \mathbb{R} \to \mathbb{R}$ be a non-decreasing and Lipschitz continuous function. Let $u \in BV(\Omega)$. Then $f(u) \in BV$ and $\partial J(u) \subset \partial J(f(u))$.*

(ii) Let $\phi : \Omega \times \mathbb{R} \to (-\infty, +\infty]$ be a measurable function. Assume that there exists a nonnegative function $\alpha \in L^1(\Omega)$, a constant $C > 0$ and $1 \le p < \infty$ such that

$$|\phi(x, s)| \le C|s|^p + \alpha(x) \tag{2.4}$$

for a.e. $x \in \Omega$ and all $s \in \mathbb{R}$. Then the functional S_ϕ is L^p continuous if and only if $\phi(x,\cdot)$ is continuous for a.e $x \in \Omega$.

Proposition 2.6. *There exist $C_1, C_2 > 0$ and $D_1, D_2 > 0$ such that*

$$\varphi(x,s) \geq C_1|s| - D_1, \qquad \psi(x,s) \geq C_2|s| - D_2 \tag{2.5}$$

for almost all $x \in \Omega$, where φ and ψ are defined as in (2.1), (2.2), the constants C_1, C_2, D_1 and D_2 are only dependent on f.

Proof. Here we only consider the first inequality in (2.5), since the proof of the second inequality is similar to the proof of the first one. In the following we will prove the result from three cases:

1. As $s < a < a_1 := \min\{0, \log f_{\min}\}$, we get that for a.e. $x \in \Omega$, there exists $\xi \in (s,a)$ such that

$$\begin{aligned}\varphi(x,s) =&\varphi(x,a) + \varphi'(x,a)(s-a) + \frac{\varphi''(\xi)}{2}(s-a)^2\\ \geq&\varphi'(x,a)s + \varphi(x,a) - \varphi'(x,a)a\\ =&-\varphi'(x,a)|s| + \varphi(x,a) - \varphi'(x,a)a.\end{aligned} \tag{2.6}$$

Furthermore, we easily obtain that for a.e. $x \in \Omega$, $\varphi'(x,a) = 2(1 - f^2(x)e^{-2a})$, thus

$$\varphi'(x,a) \leq 2(1 - {f_{\min}}^2 e^{-2a}) < 2(1 - {f_{\min}}^2 e^{-2a_1}) \leq 0.$$

On the other hand, since $\varphi(x,a) - \varphi'(x,a)a \in L^\infty(\Omega)$, we get that there exists a constant $D_1 > 0$ such that for almost all $x \in \Omega$,

$$\varphi(x,a) - \varphi'(x,a)a \geq -D_1.$$

Hence, by using (2.6) and taking $C_1 = -2(1 - {f_{\min}}^2 e^{-2a}) > 0$, we can get that the first inequality holds.

2. As $s > b > b_1 := \max\{0, \log f_{\max}\}$, we get that for a.e. $x \in \Omega$, there exists $\zeta \in (b,s)$ such that

$$\begin{aligned}\varphi(x,s) =&\varphi(x,b) + \varphi'(x,b)(s-b) + \frac{\varphi''(\zeta)}{2}(s-b)^2\\ \geq&\varphi'(x,b)s + \varphi(x,b) - \varphi'(x,b)b\\ =&\varphi'(x,b)|s| + \varphi(x,b) - \varphi'(x,b)b.\end{aligned} \tag{2.7}$$

Notice that for a.e. $x \in \Omega$,

$$\varphi'(x,b) = 2(1 - f^2 e^{-2b}) \geq 2(1 - {f_{\max}}^2 e^{-2b}) > 2(1 - {f_{\max}}^2 e^{-2b_1}) \geq 0.$$

On the other hand, since $\varphi(x,b) - \varphi'(x,b)b \in L^\infty(\Omega)$, we get that there exists a constant $D_1 > 0$ such that for almost all $x \in \Omega$,

$$\varphi(x,b) - \varphi'(x,b)b \geq -D_1.$$

Hence, by using (2.7) and taking $C_1 = 2(1 - {f_{\max}}^2 e^{-2b}) > 0$, we also get the first inequality.

3. As $s \in [a,b]$, we also get that for a.e. $x \in \Omega$,

$$\begin{aligned}\varphi(x,s) =&\varphi(x,0) + \varphi'(x,0)s + \frac{\varphi''(\eta)}{2}s^2\\ \geq&\varphi'(x,0)s + \varphi(x,0)\\ =&2s - 2f^2 s + \varphi(x,0),\end{aligned}$$

where η is between 0 and s.

If $s > 0$, by taking $C_1 = 2$ and choosing $D_1 > 0$ such that $-2f^2s + \varphi(x,0) \geq -D_1$ for almost all $x \in \Omega$ and $s \in [a,b]$, we can get the first inequality.

If $s < 0$, from (2.8) we obtain that

$$\begin{aligned}\varphi(x,s) &\geq 2f^2|s| + 2s + \varphi(x,0)\\ &\geq 2{f_{\min}}^2|s| + 2s + \varphi(x,0).\end{aligned}$$

Therefore, by by taking $C_1 = 2{f_{\min}}^2$ and choosing $D_1 > 0$ such that $2s + \varphi(x,0) \geq -D_1$ for almost all $x \in \Omega$ and $s \in [a,b]$, we also get the first inequality. □

3 The Variational Problems

In this section we study the following variational problems:

$$\inf_{w \in BV(\Omega)} \{T_\varphi(w)\}, \tag{3.1}$$

$$\inf_{u \in BV(\Omega)} \{T_\psi(u)\}, \tag{3.2}$$

where T_φ, T_ψ are defined as in (2.3).

In fact, in [12] we had already given a proof of the existence and uniqueness of the minimizer to the variational Problem (3.2). For the completion of this paper, we give a new proof of the existence and uniqueness of the minimizers for the variational Problems (3.1) and (3.2). First, we give the following lemma.

Lemma 3.1. *Let $f \in L^\infty(\Omega)$ with $f_{min} > 0$. Then the functionals T_φ and T_ψ are BV-coercive.*

Proof. We only prove the case for T_φ, since the following arguments are same for T_φ and T_ψ. The Pnoincaré inequality yields that there exists a constant $C > 0$ such that

$$\|w - \overline{w}\|_{L^1} \leq CJ(w),$$

where $\overline{w} := \frac{1}{|\Omega|}\int_\Omega w(x)dx$ and $|\Omega|$ denotes the Lebesgue of Ω. Furthermore, we get

$$\|w\|_{L^1} \leq \|w - \overline{w}\|_{L^1} + |\overline{w}||\Omega|.$$

Thus we have

$$\|w\|_{BV} \leq (C+1)J(u) + |\overline{w}||\Omega| \leq CT_\varphi(w) + |\overline{w}||\Omega|. \tag{3.3}$$

On the other hand, by using (2.5) we obtain

$$S_\varphi(w) \geq C_1 \int_\Omega |w(x)|dx - D_1|\Omega| \geq |\Omega|(C_1|\overline{w}| - D_1)$$

and thus

$$|\overline{w}| \leq \frac{1}{C_1|\Omega|}S_\varphi(w) + \frac{D_1}{C_1} \leq \frac{1}{C_1|\Omega|}T_\varphi(w) + \frac{D_1}{C_1}. \tag{3.4}$$

Combining (3.3) and (3.4), we get

$$\|w\|_{BV} \leq C_3T_\varphi(w) + C_4.$$

Therefore, T_φ is BV-coercive. □

Theorem 3.2. *Assume that $f \in L^\infty(\Omega)$ with $f_{\min} > 0$. Then there exists a unique minimizer to the variational Problems (3.1) and (3.2), respectively.*

Proof. Since S_φ and S_ψ are proper and strictly convex, by using Theorem 2.1, we can easily check that the functionals T_φ and T_ψ are proper strictly convex and lower semi-continuity. On the other hand, by Lemma (3.1) we know that T_φ and T_ψ are BV-coercive. Hence, by the direct method of the calculus of variations[7] there exists a minimizer to the both variational problems which is unique due to the strict convexity of T_φ and T_ψ. □

In the rest of this section, we give the following theorem to clarify the relation between the minimizer of (3.1) and the minimizer of (3.2). Motivated by the work in [19], we apply Γ-convergence arguments to get the proof of the following theorem.

Theorem 3.3. *Let $f \in L^\infty(\Omega)$ with $f_{\min} > 0$ and $\lambda_2 = 2\lambda_1$. Then $\widehat{w}$ is the minimizer of (3.1) if and only if $\widehat{u} = e^{\widehat{w}}$ is the minimizer of (3.2).*

Proof. It is only to show that $\widehat{w} = \operatorname{argmin} T_\varphi(w)$ implies $e^{\widehat{w}} = \operatorname{argmin} T_\psi(u)$, since the reverse direction follows that the minimizers are unique. In order to get this result, we proceed as follows:

(i) Choose a sequence of increasing intervals $[a_k, b_k] \subset [a_{k+1}, b_{k+1}]$ such that $\bigcup_k [a_k, b_k] = \mathbb{R}$ and $a_k < \min\{0, \log(f_{\min})\}$, $b_k > \max\{0, \log(f_{\max})\}$ for all $k \in \mathbb{N}$. Define

$$\mu_k(x) := 1 - f^2(x)e^{-2a_k}, \qquad \nu_k(x) := 1 - f^2(x)e^{-2b_k}$$

and $\mu_k := \text{ess}\ \inf_x \mu_k(x)$, $\nu_k := \text{ess}\ \sup_x \mu_k(x)$. It is easy to check that $\mu_k(x), \nu_k(x) > 0$ for a.e. $x \in \Omega$. Now we define the truncated continuous integrands for a.e. $x \in \Omega$ by

$$\varphi_k(x,s) := \begin{cases} \varphi(x,a_k) + \mu_k(x)(s - a_k), & \text{if } s < a_k, \\ \varphi(x,s), & \text{if } s \in [a_k, b_k], \\ \varphi(x,b_k) + \nu_k(x)(s - b_k), & \text{if } s > b_k, \end{cases} \tag{3.5}$$

$$\psi_k(x,s) := \begin{cases} \psi(x,e^{a_k}) + \mu_k(x)(s - e^{a_k}), & \text{if } s < e^{a_k}, \\ \psi(x,s), & \text{if } s \in [e^{a_k}, e^{b_k}], \\ \psi(x,e^{b_k}) + \nu_k(x)(s - e^{b_k}), & \text{if } s > e^{b_k}. \end{cases} \tag{3.6}$$

We also get that $\partial\ \varphi_k(x,w) = 2\partial\ \psi_k(x,e^w)$ holds for a.e. $x \in \Omega$ and any $k \in \mathbb{N}$. Furthermore, define the functionals

$$T_{\varphi,k}(w) := J(w) + \lambda_1 S_{\varphi_k}(w), \qquad T_{\psi,k}(u) := J(u) + \lambda_2 S_{\psi_k}(u).$$

For any $k \in \mathbb{N}$, these functionals are proper, convex and lower semicontinuous. In addition, by the same argument as in the proof Lemma 3.1, we obtain that for all $k \in \mathbb{N}$,

$$T_{\varphi,k}(w) \geq C_1\|w\|_{BV} - D_1, \qquad T_{\psi,k}(u) \geq C_1\|u\|_{BV} - D_1 \tag{3.7}$$

for some $C_1, C_2, D_1, D_2 > 0$. From (3.7) we see that the functionals are equi-coercive on BV. Hence, there exist minimizer $\widehat{w}_k$ and $\widehat{u}_k$ to $T_{\varphi,k}$ and $T_{\psi,k}$, respectively.

Define

$$h_k(s) := \begin{cases} e^{a_k} + e^{a_k}(s - a_k), & \text{if } s < a_k, \\ e^s, & \text{if } s \in [a_k, b_k], \\ e^{b_k} + e^{b_k}(s - b_k), & \text{if } s > b_k, \end{cases}$$

Notice that this truncated exponential function is a non-decreasing Lipschitz continuous function. Therefore, according to Proposition 2.6 (i) we get that

$$\partial J(w) \subset \partial J(h_k(w)) \tag{3.8}$$

for all $w \in BV(\Omega)$. Furthermore, by straightforward computation we can deduce that $\partial\varphi_k(x,w) = 2\partial\ \psi_k(x,h_k(w))$ so that

$$\partial S_{\varphi_k}(w) = 2\partial S_{\psi_k}(h_k(w)). \tag{3.9}$$

On the other hand, since $f \in L^\infty$ with $f_{\min} > 0$, for any given $k \in \mathbb{N}$ the function φ_k fulfills condition (2.4) with $C_k := \max\{|\mu_k|, |\nu_k|\}$, $p = 1$ and $\alpha_k := \varphi(\cdot,0) \in L^1(\Omega)$, by Proposition 2.6 (ii) we get that S_{φ_k} is continuous on L^1 (and on BV). Thus, according to Proposition 5.6 in [5], we have that

$$\partial T_{\varphi,k}(w) = \lambda_1 \partial S_{\varphi_k}(w) + \partial J(w). \tag{3.10}$$

Hence, combining (3.8)–(3.10), we obtain as $\lambda_2 = 2\lambda_1$ that

$$\partial T_{\varphi,k}(w) \subset \lambda_2 \partial S_{\psi_k}(h_k(w)) + \partial J(h_k(w)) \subset \partial T_{\psi,k}(h_k(w)).$$

Note that $\widehat{w}_k$ is a minimizer to $T_{\varphi,k}$ iff $0 \in \partial T_{\varphi,k}(\widehat{w}_k)$. Therefore, we see that if $\widehat{w}_k$ is a minimizer to $T_{\varphi,k}$, then $\widehat{u}_k = h_k(\widehat{w}_k)$ is a minimizer to $T_{\psi,k}$.

(ii) From (3.5) and (3.6) we see that the sequences $\{\varphi_k(x,w)\}_k$ and $\{\psi_k(x,u)\}_k$ are increasing sequences of nonnegative functions and for a.e. $x \in \Omega$,

$$\lim_{k\to\infty} \varphi_k(x,w(x)) = \varphi(x,w(x)),$$
$$\lim_{k\to\infty} \psi_k(x,u(x)) = \psi(x,u(x)).$$

Therefore, we get that $\{T_{\varphi,k}\}_k$ and $\{T_{\psi,k}\}_k$ are increasing sequences of nonnegative functions, and by the by the Monotone Convergence Theorem we have

$$\lim_{k\to\infty} S_{\varphi_k} = S_\varphi, \qquad \lim_{k\to\infty} S_{\psi_k} = S_\psi.$$

Hence, by Theorem 2.3 (ii) we obtain that

$$\begin{aligned} \Gamma - \lim_{k\to\infty} T_{\varphi,k} &= \lim_{k\to\infty} T_{\varphi,k} = T_\varphi, \\ \Gamma - \lim_{k\to\infty} T_{\psi,k} &= \lim_{k\to\infty} T_{\psi,k} = T_\psi. \end{aligned} \tag{3.11}$$

Note that the functionals $T_{\varphi,k}$ and $T_{\psi,k}$ are equi-coercive. By the Γ-convergence and Theorem 2.4 we get that $T_{\varphi,k}(\widehat{w}_k) \to T_\varphi(\widehat{w})$ and $T_{\psi,k}(h_k(\widehat{w}_k)) \to T_\psi(\widehat{u})$, and that $\widehat{w}_k \to \widehat{w}$, $h_k(\widehat{w}_k) \to \widehat{u}$ in $BV(\Omega)$. Thus $\widehat{w}_k$ and $h_k(\widehat{w}_k)$ converge in $L^1(\Omega)$ to $\widehat{w}$ and $\widehat{u}$ respectively. Further, there exists a subsequence $\{\widehat{w}_n\}$ which converges a.e. to $\widehat{w}$. Then by the construction of h_n, we deduce that $h_n(\widehat{w}_n)$ converges a.e. to $e^{\widehat{w}}$. On the other hand, we know that $h_n(\widehat{w}_n)$ converges in L^1 to $\widehat{u}$. Thus we get that $\widehat{u} = e^{\widehat{w}}$ a.e. in Ω. □

4 Numerical Methods and Experimental Results

In [12] some numerical tests on the JY model is demonstrated for multiplicative noise removal by using the gradient descent method. As is well known, this method is relatively slow. In this section we design a fast algorithm to solve the JY model by applying the split Bregman technique[10].

The split Bregman method solves a minimization problem by operator splitting and then applying Bregman iteration to the split problem. For the JY model, the split problem is given by

$$\min_{\vec{d},z,u} \Big\{ \int_\Omega |\vec{d}(x)| dx + \lambda_2 \int_\Omega \frac{(f-z)^2}{z} dx \Big\}$$

subject to the constraints $\vec{d} = \nabla u$ and $z = u$. In the following, we will use the Bregman iteration to solve this split problem by considering the following problem:

$$\min_{\vec{d},z,u} \Big\{ \int_\Omega |\vec{d}(x)|dx + \lambda_2 \int_\Omega \frac{(f-z)^2}{z} dx + \frac{\gamma_1}{2}\|\vec{d} - \nabla u - b_1\|_2^2 + \frac{\gamma_2}{2}\|z - u - b_2\|_2^2 \Big\}, \tag{4.1}$$

where the additional terms are quadratic penalties enforcing the constraints, b_1 and b_2 are variables related to the Bregman iteration algorithm. Further, the solution of (4.1) is obtained by solving the following three variable subproblem:

(1) **The $\vec{\mathbf{d}}$ subproblem**, with z and u fixed, is

$$\vec{d}^{n+1} = \operatorname{argmin}_u \Big\{ \int_\Omega |\vec{d}^n| dx + \frac{\gamma_1}{2}\|\vec{d}^n - \nabla u^n - b_1^n\|_2^2 \Big\}.$$

Its solution can be computed by

$$\vec{d}^{n+1} = \frac{\nabla u^n + b_1^n}{|\nabla u^n + b_1^n|} \max \Big\{ |\nabla u^n + b_1^n| - \frac{1}{\gamma}, 0 \Big\},$$

with

$$b_1^{n+1} = b_1^n + \nabla u^n - \vec{d}^n.$$

(2) **The z subproblem**, with $\vec{d}$ and u fixed, is

$$z^{n+1} = \operatorname{argmin}_z \Big\{ \lambda_2 \int_\Omega \frac{(f - z^n)^2}{z^n} dx + \frac{\gamma_2}{2}\|z^n - u^n - b_2^n\|_2^2 \Big\}.$$

Since the above objective function is strictly convex for z as $z > 0$, the solution can be solved very efficiently by using the Newton method. Here b_2^n is computed by

$$b_2^{n+1} = b_2^n + u^n - z^n.$$

(3) **The u subproblem**, with $\vec{d}$ and z fixed, is

$$u^{n+1} = \operatorname{argmin}_u \Big\{ \frac{\gamma_1}{2}\|\vec{d}^n - \nabla u^n - b_1^n\|_2^2 + \frac{\gamma_2}{2}\|z^n - u^n - b_2^n\|_2^2 \Big\}.$$

The solution u^{n+1} satisfies

$$\frac{\gamma_2}{\gamma_1} u^{n+1} - \triangle u^{n+1} = \frac{\gamma_2}{\gamma_1}(z^n - b_2^n) - \operatorname{div}(\vec{d}^n - b_1^n),$$

which is a sparse, symmetric positive definite linear system. The solution can be efficiently approximated by Gauss-Sidel iteration.

Finally, by incorporating the split Bregman technique we solve the JY model with the following algorithm:

• Initialize $u^0 = z^0 = {b_2}^0 = 0$, $\vec{d}^0 = {b_1}^0 = 0$;

• u^n, z^n, $\vec{d}^n$, ${b_1}^n$, ${b_2}^n$ are computed;

• u^{n+1} is given by solving the u subproblem, $\vec{d}^{n+1}$ and $b_1 n + 1$ are given by solving the $\vec{d}$ subproblem, z^{n+1} and b_2^{n+1} are given by solving the z subproblem;

• Check the stopping criteria, if satisfied, stop; else, $n \leftarrow n + 1$ and repeat.

The parameters are chosen as follows: $\gamma_1 = 5$, $\gamma_2 = 8$, and the larger the noise is, the smaller the fidelity coefficient λ_2 is. For the reference, the values of λ_2 are set to be in [1,2] and shown in Table 2. We remark that such simple scheme may not provide optimal parameters with respect to SNR and ReErr. Below we can demonstrate that it is effective enough to generate high-quality denoised images compared with the gradient descent method[12] where its corresponding optimal parameters are chosen.

In order to show the the efficiency of our algorithm, in the following numerical experiments we also compute the solution of the JY model by using the gradient descent method as presented in [12]. This method is given by using the following explicit iterative scheme:

$$u^{n+1} = u^n + dt\Big[\mathrm{div}\Big(\frac{\nabla u^n}{\sqrt{|\nabla u^n|^2+\delta}}\Big) + \lambda_2^n\Big(\frac{f^2}{(u^n)^2} - 1\Big)\Big],$$

where δ is set to be 10^{-4}, dt is set to be a small positive number to ensure the convergence of the iterative scheme, λ^n can be automatically updated as explained in [12]. In our experiments, the stopping criterion of both the proposed method and the gradient descent method is chosen as

$$\frac{\|u^{n+1} - u^n\|_2}{\|u^n\|_2} < 10^{-4}.$$

The following experiments are implemented with MATLAB7.8 on a core2 personal computer, 2.40GHz, 2GB RAM. The synthetic ultrasound speckle images are constructed based on the form (1.5). For the emulated experiments, a signal to noise ratio (SNR) and a relative error (ReErr) of a restored image are used to measure the quality of the restoration. For a given clean image u and its noisy observation u_0, denote by $n = u_0 - u$. With this we define the SNR and the ReErr as follows:

$$\mathrm{SNR} = 10\log_{10}\Big(\frac{\int_\Omega (u_0 - \overline{u}_0)^2 dxdy}{\int_\Omega (n - \overline{n})^2 dxdy}\Big),$$

$$\mathrm{ReErr} = \frac{\|n\|_2^2}{\|u\|_2^2},$$

where

$$\overline{u}_0 = \frac{1}{|\Omega|}\int_\Omega u_0 dxdy, \qquad \overline{n} = \frac{1}{|\Omega|}\int_\Omega n dxdy.$$

For these two criterions, the higher value of SNR and the lower value of ReErr are, the higher quality of the restored image is.

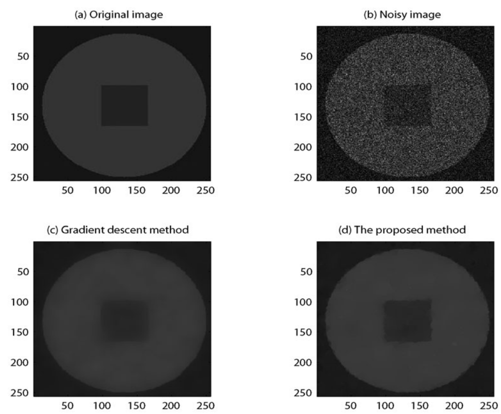

Figure 1. (a) the synthetic image "SynImag1"; (b) the multiplicative noise is added following (1.5) with the standard deviation $\sigma = 4$, SNR=1.26, ReErr=0.46.

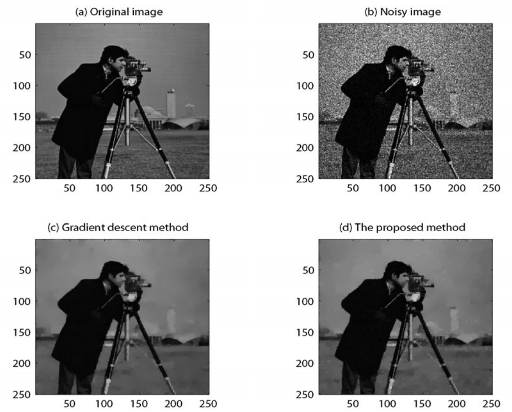

Figure 2. (a) the original “Cameraman” image; (b) the multiplicative noise is added following (1.5) with the standard deviation $\sigma = 3$, SNR=6.37, ReErr=0.25.

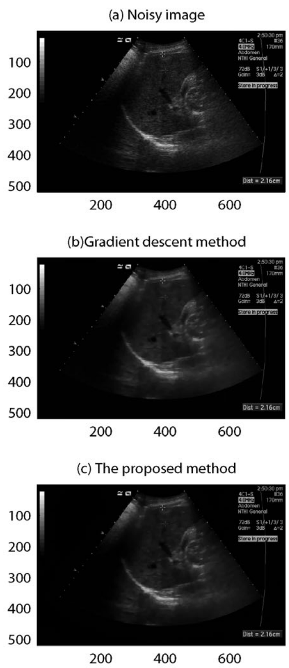

Figure 3. The real ultrasound image is restored by gradient descent algorithm and the proposed algorithm.

In Figures 1–2, a synthetic images and a real image are corrupted by the multiplicative noises following the formulation (1.5). We see from these figures that the proposed method gets a very good visual effect and recover image edges well. In Figure 3, we test speckle reduction capability of our method for a real ultrasound image. We also see that the proposed method can effectively remove the speckle noise in the ultrasound image.

We see from Table 1 that the SNRs of the images restored by the proposed method are higher than those by the gradient descent method, and the ReErrs of the images restored by the proposed method are lower than those by the gradient descent method.

In addition to the quality of the restored images, we also find that the proposed algorithm is quite efficient. Table 2 shows the number of iterations required for convergence and the computational times required by the proposed method and the gradient descent method. According to this table, we see that the proposed algorithm is much faster than the gradient descent algorithm.

Table 1. The SNRs and ReErrs of the restored images by gradient descent algorithm and the proposed algorithm

Image	Gradient descent method	Proposed method
"SynImag1" in Figure 1	SNR=11.69, ReErr=0.105	SNR= 14.84, ReErr=0.103
"Cameraman" in Figure 2	SNR=13.39, ReErr=0.096	SNR=14.01, ReErr=0.093

Table 2 The number of iterations and computational times of two methods

Image	Gradient descent method	Proposed method	Parameter
Figure 1	719 iterations 113.62 seconds	55 iterations 6.28 seconds	$\lambda_2 = 1$
Figure 2	355 iterations 46.60 seconds	59 iterations 5.49 seconds	$\lambda_2 = 2$
Figure 3	98 iterations 30.80 seconds	30 iterations 9.64 seconds	$\lambda_2 = 2$

5 Conclusion

In this paper, we have studied the relation of two variational models for speckle reduction of ultrasound images. We have shown that the solutions of these two models are equivalent as the weighted coefficients satisfy some conditions. Furthermore, we employ the split Bregman technique to propose a fast algorithm to solve one of the two models. Our experimental results have shown that the quality of images restored by the proposed method is quite good and the proposed algorithm is also quite efficient.

6 Appendix

By taking the log of both sides of (1.1), we have

$$\log f = \log u + \log n.$$

Denote by $g = \log f$, $w = \log u$ and $v = \log n$, then the new noise v satisfies the following additive noise model:

$$g = w + v.$$

In the following, let us denote by p_X the density function of random variable X. Assume that W and $V = \log N$ are independent randan variables and denote by

$$G = W + V. \tag{6.1}$$

Here we considered the discretized images, and denote by $\mathcal{S}$ the set of pixels of the image. Moreover, we assume that the samples of the noise on each pixels $s \in \mathcal{S}$ are mutually independent and identically distributed (i.i.d).

Suppose that the multiplicative noise n follows the Rayleigh law with $\sigma = \frac{1}{\sqrt{2}}$, and with density function:

$$p_N(n) = 2n \exp(-n^2). \tag{6.2}$$

It is straightforward to deduce that the density function of the random variable $V = \log N$ is

$$p_V(v) = p_N(e^v)e^v = 2e^{2v} \exp(-e^{2v}). \tag{6.3}$$

In fact, the new noise v follows a Fisher-Tippett (F-T) distribution. More details about the derivation of this distribution can be found in [4,20]. Using (6.1) and (6.3), we can easily get

$$p_{G|W}(g|w) = p_V(g - v) \ = 2e^{2(g-w)} \exp(-e^{2(g-w)}). \tag{6.4}$$

We also assume that U follows a Gibbs prior:

$$p_U(u) = \frac{1}{A} \exp(-\gamma\phi(u)), \tag{6.5}$$

where A and γ are constants, ϕ is a non-negative given function. Now given the variable G, our aim is to maximize $P(U|G)$. Applying Beyes's rule, we get $P(U|G) = \frac{P(G|U)P(U)}{P(G)}$. Thus, maximizing $P(U|G)$ amounts to minimizing the log-likelihood:

$$-\log P(W|G) = -\log P(G|W) - \log P(W) + \log P(G). \tag{6.6}$$

Notice that the samples of the noise on each pixel $s \in \mathcal{S}$ are mutually independent and identically distributed with density p_V. Therefore, we have $P(G|W) = \prod_{s\in\mathcal{S}} P(G(s)|W(s))$. Moreover, since $\log P(G)$ is a constant, we just need to minimize

$$-\log P(G|W) - \log P(W) = -\sum_{s\in\mathcal{S}} \big(\log P(G(s)|W(s)) + \log P(W(s))\big). \tag{6.7}$$

By using (6.4)–(6.7), we finally see that minimizing $-\log P(W|G)$ amounts to minimizing

$$\sum_{s\in\mathcal{S}} \big(2W(s) + e^{2(G(s)-W(s))} + \gamma\varphi(W(s))\big).$$

Here we adopt the standard TV regularizer[17], that is we choose $\varphi(w) = |\nabla w|$. Therefore, the previous computations lead to the following variational model:

$$\widehat{w} = \text{argmin}_w \Big\{ \int_\Omega |Dw| + \lambda_1 \int_\Omega (2w + e^{2(g-w)}) \Big\}, \tag{6.8}$$

where $\lambda = \frac{1}{\gamma} > 0$. By substituting e^{2g} by f^2 in (6.8) and then using $u = e^w$, we get the SO Model (1.4).

References

[1] Aubert, G., Aujol, J.F. A variational approach to removing multiplicative noise. *SIAM J. Appl. Math.*, 68: 925–946 (2008)

[2] Bioucas-Dias, J.M. Figueiredo. Multiplicative Noise Removal Using Variable Splitting and Constrained Optimization. *IEEE Transactions on Image Processing*, 19(7): 1720–1730, (2010)

[3] Darbon, J., Sigelle, M., Tupin, F. A Note on Nice-Levelable MRFs for SAR Image Denoising with Contrast Preservation. Technical Report, 2006

[4] Dutt, V., Greenleaf, J. Statistics of the Log-Compression Envelope. *Journal of Acoustical Society of America*, 99(6): 3817–3825 (1996)

[5] Ekeland, I., Témam, R. Convex Analysis and Variational Problems. SIAM, Philadelphia, 1999

[6] Maso, G.D. An introduction to Γ-convergence. Birkhäuser, Boston, 1993
[7] Evans, L.C. Partial differential equations. American Mathematical Society, 1998
[8] Evans, L.C., Gariepy, R.F. Measure Thoery and Fine Properties of Functions. CRC Press, 1992
[9] Giusti, F. Minimal Surfaces and Functions of Bounded Variation, Monographs in Math., Vol.80, Brikhäuser, Basel, 1984
[10] Goldstein, T., Osher, S. The split Bregman method for L^1 regularized problems. *SIAM Journal on Imaging Sciences*, 2(2): 323–343 (2009)
[11] Huang, Y., Ng, M., Wen, Y. A new total variation method for multiplicative noise removal. *SIAM Journal on Imaging Science*, 2(1): 20–40 (2009)
[12] Jin, Z.M., Yang, X.P. A Variational Model to Remove the Multiplicative Noise in Ultrasound Images. *Journal of Mathematical Imaging and Vision*, 39: 62–74 (2011)
[13] Kaplan, D., Ma, Q. On the statistical characteristics of the log-compressed rayleigh signals: Theorical formulation and experimental results. *J. Acoust. Soc. Amer.*, 95: 1396–1400 (1994)
[14] Lin, F.H., Yang, X.P. Geometric measure theory-an introduction. Science Press and International Press, Beijing, Boston, 2002
[15] Loupas, A. Digital image processing for noise reduction in medical ultrasonics. PhD Thesis, University of Edinburgh, UK, 1988
[16] Rudin, L., Lions, P.L., Osher, S. Multiplicative denoising and deblurring: Theory and algorithms. In: S. Osher and N. Paragios, editors, Geometric Level Sets in Imaging, Vision, and Graphics, Springer-Verlag, 2003, 103–119
[17] Rudin, L., Osher, S., Fatemi, E. Nonlinear total variation based noise removal algorithms. *Physica D*, 60: 259–268 (1992)
[18] Shi, J., Osher, S. A nonlinear inverse scale space method for a convex multiplicative noise model. *SIAM J. Imaging Sciences*, 1: 294–321 (2008)
[19] Steidl, G., Teuber, T. Removing multiplicative noise by Douglas-Rachford splitting methods. *Journal of Mathematical Imaging and Vision*, 36: 168–184 (2010)
[20] Thijssen, J.M., Oosterveld, B.J., Wanger, R.F. Gray level transforms and lesion detectabivity in echographic images. *Utrason. Imag.*, 10: 171–195 (1988)
[21] Tuthill, T.A., Sperry, R.H., Parker, K.J. Deviation from Rayleigh statistics in ultrasonic spekle. *Ultrason. Imag.*, 10: 81–90 (1988)